Younger Dryas Glaciers and climate in the Mourne Mountains, Northern Ireland

Published in:
Journal of Quaternary Science

Document Version:
Peer reviewed version

Queen's University Belfast - Research Portal:
Link to publication record in Queen's University Belfast Research Portal

Younger Dryas Glaciers and climate in the Mourne Mountains, Northern Ireland

Iestyn, D. Barr[a]*, Sam Roberson[b], Rory Flood[c], Jason Dortch[d]

[a]School of Natural and Built Environment, Queen's University Belfast, BT7 1NN, UK
[b]Geological Survey of Northern Ireland, Dundonald House, Upper Newtownards Rd, Belfast, BT4 3SB, UK
[c]School of Natural Sciences, Trinity College Dublin, Dublin 2, Ireland.
[d]Department of Geography, University of Manchester, Oxford Road, Manchester, M13 9PL, UK

*Corresponding author
Address: School of Natural and Built Environment, Queen's University Belfast, BT7 1NN, UK
Email: i.barr@qub.ac.uk
Tel: +44 (0)28 9097 5146

Abstract
Here, we present evidence to suggest that the Mourne Mountains, Northern Ireland, were last occupied by glaciers during the Younger Dryas Stadial. The margins of these glaciers are marked by moraines, chronologically constrained to the Younger Dryas by Schmidt Hammer exposure dating. Reconstructions indicate that these glaciers had equilibrium-line altitudes (ELAs) ranging from 356 ± 33 m (a.s.l.) to 570 ± 9 m (a.s.l.), with a mean of 475 ± 36 m (a.s.l.). ELAs rise from west to east, likely reflecting the contribution of windblown snow and ice to the accumulation of Younger Dryas glaciers in the western Mournes. Taking this into consideration, a mean 'climatic' ELA of 529 ± 4 m (a.s.l.) is calculated for the mountains as a whole. Assuming a mean annual sea level air temperature of -8°C, and an annual temperature range of 34°C, degree-day modelling suggests that during the Younger Dryas, accumulation at the 'climatic' ELA of glaciers in the Mournes was 846–990 mm a^{-1}. This suggests increased aridity, relative to present, and is consistent with other parts of NW Europe, where reduced precipitation, alongside notable cooling is thought to reflect increased North Atlantic sea ice extent during the Younger Dryas.

Introduction
During the Younger Dryas Stadial (known in Ireland as the Nahanagan Stadial), equivalent to Greenland Stadial-1 (GS-1; c. 12.9–11.7 ka) (Lowe *et al*., 2008), ice masses developed in many mountain ranges in NW Europe in response to rapid climatic cooling during the final stages of deglaciation from the Last Glacial Maximum (LGM) (Fairbanks, 1990; Renssen *et al*., 2015). In many parts of Scotland, Wales, England, and Ireland, the extent of these glaciers, and the climate that allowed their formation, has been the focus of considerable study (e.g., Harrison *et al*., 2010; Bendle and Glasser, 2012; Boston *et al*., 2015). However, in Northern Ireland, though there is palaeoenvironmental evidence for cooling (e.g., Watson *et al*., 2010; Walker *et al*., 2012), climatic conditions and the extent of glaciers during the Younger Dryas remain

poorly understood (see Wilson 2004a,b; Rea and McCarron, 2008). One location where glaciers are presumed to have developed is in the Mourne Mountains (hereafter 'the Mournes') (Fig. 1), where geomorphological evidence suggests the former presence of small ice masses (Sutton, 1998; Wilson, 2004a). Analysing these former glaciers has important implications for understanding local and regional palaeoclimate, since the Mournes are located between the mountains of Scotland, NW England, North Wales, and western and eastern Ireland, where glacier-based climate reconstructions for the Younger Dryas have been generated (Ballantyne *et al*., 2008; Golledge, 2010; Golledge *et al*., 2010; Harrison *et al*., 2010; Bendle and Glasser, 2012; Brown *et al*., 2013). Given this significance, the purpose of this paper is to investigate the extent of glaciers in the Mournes during the Younger Dryas, and to reconstruct the climatic conditions under which they formed.

Study area and glacial history
The Mournes are located in NE Ireland, bordering the Irish Sea Basin (Fig. 1), they cover ~ 150 km^2, and reach a maximum altitude (Slieve Donard) of 850 m above sea level (a.s.l.). The mountains are primarily composed of a granite complex that was intruded into Silurian greywacke and slate country rock c. 56 Ma (Cooper and Johnston, 2004) (Fig. 1B), and have undergone multiple phases of glaciation during the Quaternary (see Dwerryhouse, 1923; Charlesworth, 1938; Stephens *et al*., 1975; Gellatly, 1985; Sutton, 1998). At the LGM, known locally as the Glenavy Stadial (Bazley, 2004), the mountains were entirely submerged by the British Irish Ice Sheet (BIIS) which reached its maximum areal extent c. 27 ka (Clark *et al*., 2012). Following the LGM, the deglaciation of the coast of NE Ireland likely occurred sometime before 18.2 ka (during the Cooley Point Interstadial) (McCabe *et al*., 2007), when the BIIS retreated north and NW, away from the Mournes. This was followed by a period of ice sheet readvance, during the Clogher Head Stadial (c. 18.2–17.4 ka); retreat during the Linns Interstadial (c. 17.4 ka); before a final readvance during the Killard Point Stadial (c. 17.2–16.6 ka) (age estimates based on McCabe *et al*., 2007, calibrated by Clark *et al*., 2012). During these phases of readvance, the ice sheet moved south, but was deflected by the Mournes, and flowed east and west around their margins, with tongues of ice extending from North to South through the mountains. Following the Killard Point Stadial, the ice sheet retreated north and, despite later readvances, never again reached the Mournes (see McCabe and Clark, 1998; McCabe and Williams, 2012). Mountain glaciers are generally considered to have last occupied the Mournes during the Younger Drays Stadial (Sutton, 1998; Wilson, 2004a), as in other parts of Ireland (Colhoun and Synge, 1980; Anderson *et al*., 1998; Harrison *et al*., 2010) and Britain (Ballantyne, 2007a,b; Golledge, 2010; Bendle and Glasser, 2012), though no detailed analysis of the dimensions of these glaciers has been conducted (c.f. Sutton, 1998).

Methods
Geomorphological mapping
In order to establish the former extent of glaciers in the Mournes, the region's glacial geomorphology was mapped from Bing aerial photographs and during field-based investigations. Though there are a number geomorphological indicators of former glaciation in the region, including erratic boulders, striations, glacially-smoothed bedrock surfaces, and roche moutonnée (Sutton, 1998; Wilson, 2004a), our focus was primarily on mapping moraines (though cirques were also mapped), on the grounds that they are the best geomorphological indicators of the dimensions of former mountain glaciers. Mapping was guided by Sutton (1998), and restricted to moraines within, or emanating from, the mountains, rather than considering the large and conspicuous moraines, which reflect former ice sheet extent, on adjacent lowlands (see Sutton, 1998; McCabe and Dunlop, 2006).

Establishing a glacial chronology

   To establish a chronology for former glaciation in the Mournes, ideally a robust cosmogenic chronology would be established. However, to our knowledge, there are no published numerical ages to constrain the chronology of former glaciation in the mountains, and moraines are difficult to group morphostratigraphically (c.f. Lukas, 2006). In the absence of these data, Schmidt hammer exposure dating (SHED) was used in the present investigation. SHED is a long established technique for obtaining a relative chronology for surface exposure (Matthews and Shakesby, 1984), and has been widely applied to glacial environments (Goudie, 2006; Tomkins *et al*., 2016). The principal of the method is that the Schmidt hammer is applied to a rock surface, and a rebound value (R) recorded. This R-value is considered a measure of rock strength—with stronger/harder surfaces returning higher R-values (Aydin and Basu, 2005). In formerly glaciated environments it is assumed that surfaces that have been glacier-free (i.e., exposed) for long periods will have experienced considerable weathering, and will therefore be 'softer', and return lower R-values, than more recently deglaciated areas. As a result, the procedure can be a simple and rapid way of establishing a relative chronology of deglaciation.

   To obtain numerical age estimates using the technique requires independent dating control to generate R-value calibration curves (i.e., to convert R-values to numerical ages) (see Winkler, 2009; Matthews and Owen, 2010). Recently, Tomkins *et al*. (2016) produced a series of R-value calibration curves by sampling 76 surfaces in the UK, dated using Beryllium-10 (^{10}Be) Terrestrial Cosmogenic Nuclide Dating (TCND). Tomkins *et al*. (2016) produced individual curves for different lithologies, but found that granite surfaces alone demonstrate a statistically significant relationship between exposure age and R-values (see Fig. 2). In the present study, this calibration curve (Fig. 2) was used to establish a chronology of deglaciation in the Mournes. To allow direct comparison with their calibration curve, sampling procedures followed Tomkins *et al*. (2016). R-value measurements were taken using a Proceq^{TM} 'N' type Schmidt Hammer. Sampling was restricted to horizontal (or near horizontal), dry surfaces on large boulders (> 1 m in length) or exposed bedrock surfaces (e.g., tors). In each case, the Schmidt hammer was held perpendicular to the surface, avoiding rough, irregular or lichen covered areas. To ensure that the sampled surfaces had been exposed to weathering continuously since deglaciation, samples were taken from sites away from cliff faces or valley walls, and in many cases sampled boulders were located on moraine crests (e.g., Fig. 3). At each location (e.g., on each moraine or summit) three surfaces and/or boulders were sampled, and, for each, 30 R-values were recorded (from numerous positions on each surface). In order to assess loss in Schmidt hammer condition over time, the same granite boulder was analysed at the beginning and end of sampling. This indicated a 2 point difference in R-values between the beginning (6 May 2016) and end of sampling (23 July 2016). By arranging the R-values chronologically, based on the date/time of collection, a correction was made assuming a linear deterioration in Schmidt hammer performance (following Tomkins *et al*., 2016). To utilise Tomkins *et al*. (2016) R-value to numerical age curve for granite, our Schmidt Hammer required calibration against the University of Manchester calibration boulder (see Dortch *et al*., 2016). This returned an average R-value of 48.70 ± 1.3, compared to the calibration value of 48.08 ± 0.82 reported by (Tomkins *et al*., 2016), and values were corrected to account for this difference.

   Despite the lack of independent dating control, a number of characteristics likely make the Mournes a suitable location for applying the SHED approach outlined above, First, the mountains are dominated by granite lithology (see Fig. 1B), meaning that the calibration curve in Fig. 2 can be directly applied. Second, the mountain range is comparatively small (~ 150 km^2) meaning that variations in climate (known to influence rock weathering rates) between sampled surfaces are likely to be minimal. Third, since the calibration curve (Fig. 2) is based

on dated surfaces from areas of the UK submerged beneath the BIIS during the LGM, and fully deglaciated by the onset of the Holocene, it is only really applicable to surfaces exposed during this period. Fortunately, the Mournes are considered to have experienced a similar glacial history to the sites sampled by Tomkins *et al.* (2016).

The granite SHED curve of Tomkins *et al.* (2016) is based on TCND, therefore SHED inherits some of the weaknesses of TCN methods. For example, rock surfaces can be exposed prior to final deposition, which would lead to a softer surface (lower R-value) and inherited TCNs. Conversely, post-depositional rock surfaces that have been exhumed or have spalled part of their surface off would lead to higher R-values and a reduced TCN concentration. Therefore, the calibrated SHED ages need to be analysed with appropriate statistics. Here, we followed the methods of Dortch *et al.* (2013) and Murari *et al.* (2014) and used the "ksdensity" kernal in MATLAB 2015a to produce probability density estimates (PDE). The PDEs were then modelled to separate out Gaussians to eliminate positive or negative skew. The highest probability Gaussian is selected with the peak and 1σ uncertainties reported, since all ages are younger than the LGM (c.f. Dortch *et al.*, 2013). Ages within 2σ that contribute to one of the selected Gaussians were compared using a two-tailed unequal-variance Student's T-Test to determine if events are different.

Glacier reconstruction

The dimensions of Younger Dryas glaciers in the Mournes were reconstructed from mapped moraines. Based on the results of SHED, all cirques in the Mournes were presumed to have been occupied by glaciers during this period. Three-dimensional reconstructions of glaciers within, and/or emanating from, these cirques were generated using the GIS tool of Pellitero *et al.* (2016). In each case, a basal shear stress of 100 kPa was applied, using a step length of 10 m (for details see Pellitero *et al.*, 2016).

Equilibrium-line altitude estimates

A glacier's equilibrium-line altitude (ELA) is defined as the altitude where net annual accumulation and ablation are equal, and is largely controlled by climate (Ohmura *et al.*, 1992). Estimating palaeo ELAs is therefore an established approach for obtaining palaeoclimatic information from glacier reconstructions (see Porter, 2001; Osmaston, 2005). In the present study, ELA was estimated using the GIS tool of Pellitero *et al.* (2015), applying the Area-Altitude Balance Ratio (AABR) method (considered the most robust method), with an AABR of 1.9 ± 0.81 (following Rea, 2009). As noted above, ELA is linked to climate, however in some instances, particularly in the case of small glaciers, ELA is also strongly influenced by non-climatic factors, such as the supply of snow and ice from indirect sources (i.e., from surrounding topography) (Kern and László, 2010). In order to assess the impact of this 'redistributed' snow and ice on the ELAs of reconstructed Younger Dryas glaciers in the Mournes, combined snow and avalanche contributing ratios were calculated (see Ballantyne, 2007a,b). This involved calculating the ratio of a glacier's potential avalanche and snow contributing area (A_c) to its total surface area (A_g) (see Ballantyne, 2007a,b). A large Ac/Ag suggests a greater potential for redistributed snow and ice to make a notable contribution to glacier accumulation. In applying this approach to the Mournes, it was assumed that snow-bearing winds during the Younger Dryas were dominantly sourced from the west/SW (210-300°), as they are today (Betts, 1997).

Links to palaeoclimate

In order to estimate the climate necessary to sustain the reconstructed Younger Dryas glaciers in the Mournes, degree-day modelling (DDM) was utilised (see Laumann and Reeh, 1993; Braithwaite *et al.*, 2006). This approach, which has been widely adopted elsewhere (e.g.,

Hughes and Braithwaite, 2008; Barr and Clark, 2011; Bendle and Glasser, 2012), involves using an independent estimate of palaeotemperature to calculate annual melt (i.e., ablation) at the ELAs of reconstructed glaciers, based on as assumed melt rate. In the DDM approach, annual melt (M_a) at a glacier's ELA is calculated as the annual sum of daily melt values (M_d). Daily melt values are calculated by multiplying positive (i.e., > 0°C) mean daily temperature (T_d) by a degree-day melt factor (DDF) (eq. 1).

$$M_d = T_d \times DDF \text{ (eq. 1)}$$

In this study a DDF of 4.1 ± 1.5 mm °C^{-1} day^{-1} was used (Braithwaite 2008). By assuming that the annual distribution of temperatures is described by a sine curve (Hughes and Braithwaite, 2008), mean daily temperature (T_d) during the Younger Dryas was calculated from eq.2., using independent estimates of mean annual temperature (T_a) and annual temperature range (A_y) during this period (both from Isarin et al., 1998).

$$T_d = A_y \sin\left(\frac{2\pi d}{\lambda} - \phi\right) + T_a \text{ (eq. 2)}$$

where A_y is the amplitude of annual temperature variability (1/2 of the annual temperature range), d the ordinal day, λ is the period (365 days), ϕ is the phase angle of the sine curve (here 1.93 radians based on the general assumption that temperature is maximal in July and minimal in January), and T_a is mean annual air temperature.

Since net annual accumulation and ablation at the ELA are considered equal, M_a calculated using this approach is considered an estimate of annual accumulation (considered a proxy for palaeoprecipitation) at the ELA of reconstructed glaciers.

Results
Geomorphology
Based on geomorphological mapping, it is apparent that distinct moraine sequences are found within, and adjacent to (within 500–1500 m), cirques in the Mournes (Fig. 1A). These upland moraines are distributed radially around the mountains, suggesting that they were deposited by mountain-centred ice masses, rather than by external ice flowing from the North. This assertion is supported by the lithology of debris within the moraines, which is predominantly comprised of locally-sourced Mourne granite (Wilson, 2004a). As such, these ridges are considered to have been deposited by former mountain- or cirque-style glaciers (Sutton, 1998; Wilson, 2004a). Lowland moraines occupy many of the region's trunk valleys (see Fig. 1A) and are widely presumed to have been deposited during the Killard Point Stadial, when larger glaciers occupied some valleys, and tongues of ice extended through the mountains from the BIIS located to the North (Sutton, 1998).

Chronology
To establish a chronology of deglaciation in the Mournes, a total of 53 separate locations (on mountain summits, cols, valleys, and cirques) were sampled for Schmidt hammer dating (see Fig. 1A). At each location, 30 R-values were recorded from 3 different surfaces (boulders or bedrock)—with measurements taken from numerous positions on each surface. Resulting SHED age estimates range from 6.5 ± 0.8 ka to 20.1 ± 1.0 ka (see supplementary information). Selected Gaussians from PDE models show a distinction between summit (15.6 ± 1.9 ka), col (14.2 ± 1.7 ka), valley (10.5 ± 1.4 ka) and cirque (8.8 ± 0.8 ka) locations (Fig. 4). The Gaussian models show a considerable amount of post-glacial exhumation or surface spallation affecting

summit and col age distributions (Fig. 4A–B). In contrast, cirque and valley age distributions are skewed by exposure prior to deposition leading to softer surfaces (Fig. 4C–D). Prior exposure is a common issue with TCND in the UK due to the lower erosivity of Younger Dryas ice. Cirque SHED age distribution is also considerably affected by exhumation or spalling of surfaces, which indicates considerable post-depositional reworking. P-values resulting from T-Tests on ages for each landform type within 2σ of the selected Gaussians are all < 0.01. This indicates that, while there is some overlap of uncertainties, the events are statistically distinguishable and separate (See table 1). The data indicate that summits deglaciated following the LGM, closely followed by cols. Valleys last deglaciated during the late glacial (during phases of ice sheet readvance) and cirques last deglaciated following the Younger Dryas. The age estimates show some relationship with altitude (R^2=0.27, P-value <0.01; Fig. 5). However, low altitude valley samples typically return older age estimates than higher altitude cirques (Fig. 5), thus the relationship likely reflects the region's glacial history, rather than an altitudinal control on the rate of post-glacial weathering (see Tomkins *et al*., 2016).

Younger Dryas glaciers and their ELAs
On the basis of the geomorphological mapping and SHED chronology, 24 Younger Dryas glaciers were reconstructed in the Mournes (see Fig. 6). In places where multiple moraines potentially mark Younger Dryas ice margins, both minimum and maximum glacier reconstructions were generated (see Fig. 6). In total, the reconstructions indicate that during the Younger Dryas, the mountains were occupied by glaciers with a total surface area of 3.42–5.24 km^2 (see Table 2). These glaciers have ELAs ranging from 356 ± 33 m (a.s.l.) to 570 ± 9 m (a.s.l.), with a mean ELA of 475 ± 36 m (a.s.l.) (Table 2). Values for individual glaciers typically rise from west to east (Fig. 7A). This trend might reflect a precipitation gradient during the Younger Dryas, however when the impact of redistributed snow and ice is considered (Mitchell, 1996; Carrivick and Brewer, 2004), results indicate that ELA and snowblow and avalanche ratios (A_c/A_g) are related (Fig. 7B–C), and that glaciers in the western Mournes (labelled 1 and 2 in Figs. 7A & B) have comparatively large snowblow and avalanche ratios. This likely reflects their position on the lee (eastern) side of an extensive (~ 6 km^2) upland plateau (Wilson, 2004a) (see Fig. 1A). This applies when both the minimum (Fig. 7B) and maximum (Fig. 7C) glacier reconstructions are considered. It is therefore possible that the plentiful supply of redistributed snow and ice explains the low ELAs of these glaciers, and that the West–East ELA gradient (Fig. 7A) is not climatically driven. Thus the reported mean ELA of glaciers in the Mournes during the Younger Dryas (i.e., 475 ± 36 m) (Table 2), is likely partly controlled by the availability of redistributed snow and ice (and cannot be directly linked to climate). In order to estimate a 'climatic' ELA, the regression lines in Fig. 7B–C can be extrapolated to simulate conditions for a hypothetical glacier receiving no accumulation from redistributed snow or ice (i.e., Ac/Ag = 0) (see Bendle and Glasser, 2012). Applying this technique in the Mournes yields a mean 'climatic' ELA of 529 ± 4 m (a.s.l.).

Degree-day model output
The DDM approach is used to predict annual accumulation in the Mournes during the Younger Dryas based on reconstructed glaciers and independent estimates of mean annual temperature and annual temperature range during this period. To simulate the coldest part of the Younger Dryas, a mean annual sea level air temperature of -8°C, and an annual temperature range of 34°C are assumed (Isarin *et al*., 1998). With a DDF of 4.1 ± 1.5 mm °C^{-1} day^{-1} (Braithwaite 2008), and an environmental lapse rate of 0.006–0.007°C m^{-1} (Bendle and Glasser, 2012), this approach predicts annual accumulation of 844–2132 mm a^{-1} at the mean 'climatic' ELA of Younger Dryas glaciers in the Mournes (Table 3).

Discussion
A deglacial chronology for the Mournes
Results from SHED in the Mournes (see supplementary information, and Fig. 4) are broadly consistent with the existing view of post-LGM glaciation in the region. Specifically, results indicate that summits were last deglaciated during ice sheet retreat from the LGM, and that the higher cols were then exposed (Fig. 4). Valleys were last deglaciated during the late glacial (likely during a phase of ice sheet readvance), and cirques were last glaciated during the Younger Dryas. Despite the evidence to support this pattern, it is notable that the age estimates derived from the SHED approach are typically younger (more recent) than suggested by 'established' chronologies (Fig. 4). However, there are few chronologies available for comparison in Norther Ireland. Alternatively, the younger ages may indicate a limitation of the SHED approach applied here. Specifically, the local climate, or local granite that is slightly different to the granites in the calibration dataset, might mean that the Schmidt hammer calibration curve of Tomkins *et al*. (2016) is not directly applicable to the Mournes—something which might be addressed by establishing an independent cosmogenic chronology, from which a local Schmidt hammer calibration curve (equivalent to Fig. 2) could be constructed. Despite this, the SHED approach differentiates between different phases of glaciation in the Mournes (Fig. 4), and is considered a viable method for constraining the extent of the region's glaciers during the Younger Dryas.

Younger Dryas climate in the Mournes
Meteorological data from Annalong (130 m a.s.l., ~54.11°N, 5.90°W) (labelled in Fig. 1A) reveals modern precipitation (AD 1931–1994) of 1227 mm a^{-1} (Peterson and Vose, 1997). Adjusted to an altitude of 529 ± 4 m (a.s.l.), and assuming a rate of precipitation increase with altitude of 3.0 mm m^{-1} (Brunsdon *et al*., 2001), yields a modern precipitation estimate of 2424 ± 12 mm a^{-1} at the 'climatic' ELA of Younger Dryas glaciers in the Mournes. By contrast, model data from the present study indicate that during the Younger Dryas, accumulation at this altitude was 844–2132 mm a^{-1}. This suggests a reduction in mean annual precipitation, relative to present. In fact, the temperature data used in the DDM (see Isarin *et al*., 1998), with notably low winter temperatures and a greater annual temperature range, suggest that the Mournes likely experienced comparatively continental conditions during the Younger Dryas. Under such conditions, model outputs based on a DDF of 2.6 (the lowest value used in the present study) might be a better representation of 'true' Younger Dryas conditions (since higher DDFs are unrepresentative of glaciers occupying continental climates—see Braithwaite *et al*., 2006; Hughes, 2009). When the model is run with a DDF of 2.6, results indicate mean accumulation of 846–990 mm a^{-1} (Table 3), suggesting notable aridity during the Younger Dryas, relative to present. Unfortunately, though independent palaeoenvironmental proxies indicate cooling, landscape instability and the expansion of arctic shrub tundra in Ireland during the Younger Dryas (Watson *et al*., 2010; Walker *et al*., 2012), there is little information about precipitation during this period against which to validate these inferences. Despite this, the precipitation values reported here are comparable to those reconstructed for the Younger Dryas in parts of central and western Scotland (see Table 5 in Boston *et al*., 2015), but generally lower than for parts of NW Wales (see Table 2 in Bende and Glasser, 2012).

Regional comparison
Modelling results from the present study suggest that Younger Dryas climate in the Mournes was continental, with particularly cold winters and reduced precipitation relative to present. Similar conditions have been proposed for other regions bordering the Irish Sea. For example, the Isle of Arran (Ballantyne, 2007a,b), Southern uplands (Cornish, 1981; Gordon, 1999), English Lake District (Sissons, 1980; Walker, 2004), and NW Wales (Bendle and Glasser,

2012), are considered to have been notably drier than present during the Younger Dryas. Bendle and Glasser (2012) note that evidence for drier conditions is generally consistent with proxy archives (e.g. Isarin and Renssen, 1999) and ice core evidence (Alley, 2000) which suggest reduced annual snowfall across NW Europe during the Younger Dryas. The consensus view is that this aridity occurred as a result of low winter temperatures causing the formation of extensive sea ice (down to ~ 50–52°N) in the North Atlantic (Renssen and Isarin, 1998; Renssen and Vandenberghe, 2003; Golledge *et al.*, 2010). Thus, conditions during this period may have been notably seasonal, with dry, arid winters (when sea ice was at its most extensive) and comparatively mild summers (Golledge, 2010; Bendle and Glasser, 2012). Under such conditions, moisture availability from the North Atlantic is considered to have been an important control on glaciation in NW Europe, with dominant westerly and southwesterly winds generating strong West–East precipitation (and associate ELA) gradients (Ballantyne, 1989; Sissons, 1979, 1980; Hughes, 2009; Golledge, 2010). For example, at Achill Island on the west coast of Ireland (~ 260 km west of the Mournes) moisture from the North Atlantic is considered to have sustained Younger Dryas glaciers with ELAs close to modern sea level (Bowen *et al.*, 2002; Ballantyne *et al.*, 2008), whereas in central and eastern Scotland ELAs were > 700 m (a.s.l.) (Boston *et al.*, 2015). Under such continental conditions, glaciers in the Mournes are likely to have been comparatively moisture-starved, and partly sustained because of a shortened ablation season, and the plentiful supply of redistributed snow and ice (Sutton, 1998). Golledge (2010) suggests that in western Scotland, extreme continental conditions during the most severe period of the Younger Dryas (with climate 6–8°C cooler than present during the summer months, but as much as 30°C colder during the winter) were unconducive to glacier growth, and that perhaps glaciers were at their most extensive during the early stages of the Younger Dryas, when temperature depression and sea-ice induced aridity were less severe (Walker *et al.*, 2003; Walker, 2004; Bendle and Glasser, 2012). This may be true for the Mournes, and might explain why sequences of moraines are found within inferred maximum Younger Dryas glacier limits (Fig. 1A)—i.e., perhaps these 'inner' moraines reflect less extensive advances and/or periods of stabilisation during overall retreat from an early Younger Dryas ice extent maximum. Similar evidence, to suggest the development of comparatively extensive glaciers during the early Younger Dryas, has been found in other regions bordering the Irish Sea (see Bendle and Glasser, 2012).

Despite the evidence for increased aridity and continentality in NW Europe during the Younger Dryas, some regions appear to indicate precipitation totals comparable to, or even greater than, present. For example, in NW Scotland, there is some evidence of increased precipitation (by up to 26%) during the Younger Dryas (Ballantyne, 1989; Benn and Lukas, 2006; Lukas and Bradwell, 2010). However, in NW Scotland elevated precipitation is partly attributable to increased storminess, combined with the local presence of the Western Highlands ice field (see Golledge, 2008), which forced westerly and southwesterly air masses to rise and cool, meaning that adjacent areas (to the west) received heavy snowfall (Sissons, 1979, 1980; Ballantyne, 2007a,b). Such conditions are unlikely to have prevailed in the Mournes, and evidence from the present study appears to support the idea that Younger Dryas climate in Northern Ireland was colder, drier, and more continental than present. In fact, it is notable that insolation at these latitudes, and atmospheric CO_2 concentrations, were relatively high during the Younger Dryas (relative to earlier cold periods) (Imbrie et al., 1984; Liu et al., 2013), but freshwater inputs, ice bergs and sea-ice acted to cool North Atlantic climate by disrupting oceanic and atmospheric circulation (Isarin et al., 1998; Bakke et al., 2009; Golledge, 2010).

Conclusions

In this study, the extent of Younger Dryas glaciers in Mourne Mountains, Northern Ireland, has been reconstructed, and used to infer regional palaeoclimate. The main study findings are summarised as follows:

1. Geomorphological mapping reveals upland moraine sequences, suggesting the former presence of cirque and valley glaciers.
2. Results of SHED appear to chronologically constrain these moraines to the Younger Dryas, and are broadly consistent with the 'established' view of post-LGM deglaciation from the Mournes—i.e., with summits and some cols last deglaciated following the LGM, valleys last deglaciated during the late glacial (during phases of ice sheet readvance) and cirques last deglaciated following the Younger Dryas.
3. On the assumption that the region's cirques were last occupied during the Younger Dryas, 24 glaciers, covering 3.42–5.24 km^2, are reconstructed for this period. These glaciers have ELAs ranging from 356 ± 33 m (a.s.l.) to 570 ± 9 m (a.s.l.), with a mean of 475 ± 36 m (a.s.l.). These ELA estimates rise from west to east, but this is considered to reflect the supply of redistributed snow and ice to glaciers occupying the western Mournes, rather than indicating a clear climatic gradient.
4. When the role of redistributed snow and ice is accounted for, a Younger Dryas 'climatic' ELA of 529 ± 4 m (a.s.l.) is calculated for the mountains.
5. Assuming mean annual sea level air temperature of -8°C and an annual temperature range of 34°C (Isarin *et al*., 1998), degree-day modelling suggests that during the Younger Dryas, annual accumulation at the 'climatic' ELA of glaciers in the Mournes was 844–2132 mm a^{-1}. However, given evidence for increased continentality in the region, annual accumulation was likely in the 846–990 mm a^{-1} range, suggesting notably increased aridity relative to present. As in other parts of NW Europe, this reduction in precipitation, alongside notable cooling (with cooling of 7.0°C in summer, and 28.2°C in winter) is thought to reflect extensive North Atlantic sea ice (suppressing evaporation) during the Younger Dryas.

References

Alley RB. 2000. The Younger Dryas cold interval as viewed from central Greenland. *Quaternary Science Reviews* **19**: 213–226.

Anderson E, Harrison S, Passmore DG, Mighall TM. 1998. Geomorphic evidence of Younger Dryas glaciation in the Macgillycuddy's Reeks, south west Ireland. *Quaternary Proceedings* **6**: 75–90.

Aydin A, Basu A. 2005. The Schmidt hammer in rock material characterization. *Engineering Geology* **81**: 1–14.

Bakke J, Lie Ø, Heegaard E, Dokken T, Haug GH, Birks HH, Dulski P, Nilsen T. 2009. Rapid oceanic and atmospheric changes during the Younger Dryas cold period. *Nature Geoscience* **2**(3): 202–205.

Ballantyne CK. 1989. The Loch Lomond Advance on the Isle of Skye, Scotland: glacier reconstruction and palaeoclimatic implications. *Journal of Quaternary Science* **4**: 95–108.

Ballantyne CK. 2007a. Loch Lomond Stadial glaciers in North Harris, Outer Hebrides, North-West Scotland: glacier reconstruction and palaeoclimatic implications. *Quaternary Science Reviews* **26**: 3134–3149.

Ballantyne CK. 2007b. The Loch Lomond Readvance on north Arran, Scotland: glacier reconstruction and palaeoclimatic implications. *Journal of Quaternary Science* **22**(4): 343–359.

Ballantyne CK, Stone JO, McCarroll D. 2008. Dimensions and chronology of the last ice sheet in Western Ireland. *Quaternary Science Reviews* **27**(3): 185–200.

Barr ID, Clark CD. 2011. Glaciers and climate in Pacific Far NE Russia during the Last Glacial Maximum. *Journal of Quaternary Science* **26**(2): 227–237.

Bazley RAB. 2004. Quaternary. In *The Geology of Northern Ireland, Our Natural Foundation*, Mitchell W (ed.). The Geological Survey of Northern Ireland: Belfast; 211–226.

Bendle JM, Glasser NF. 2012. Palaeoclimatic reconstruction from lateglacial (younger dryas chronozone) cirque glaciers in snowdonia, north wales. *Proceedings of the Geologists' Association* **123**(1): 130–145.

Benn DI, Lukas S. 2006. Younger Dryas glacial landsystems in North West Scotland: an assessment of modern analogues and palaeoclimatic implications. *Quaternary Science Reviews* **25**: 2390–2408.

Betts, N., 1997. Climate. In *Soil and Environment: Northern Ireland*, Cruickshank JG (ed.). Agricultural and Environmenral Science Division: Queen's University Belfast.

Boston CM, Lukas S, Carr SJ. 2015. A Younger Dryas plateau icefield in the Monadhliath, Scotland, and implications for regional palaeoclimate. *Quaternary Science Reviews* **108**: 139–162.

Bowen DQ, Phillips FM, McCabe AM, Knutz PC, Sykes GA. 2002. New data for the last glacial maximum in Great Britain and Ireland. *Quaternary Science Reviews* **21**: 89–101.

Braithwaite RJ. 2008. Temperature and precipitation climate at the equilibrium line altitude of glaciers expressed by the degree-day factor for melting snow. *Journal of Glaciology* **54**: 437–444.

Braithwaite RJ, Raper SCB, Chutko K. 2006. Accumulation at the equilibrium line altitude of glaciers inferred from a degree–day model and tested against field observations. *Annals of Glaciology* **43**: 329–334.

Brown VH, Evans, DJ, Vieli A, Evans IS. 2013. The Younger Dryas in the English Lake District: reconciling geomorphological evidence with numerical model outputs. *Boreas* **42**(4): 1022–1042.

Brunsdon C, McClatchey J, Unwin DJ. 2001. Spatial variations in the average rainfall–altitude relationship in Great Britain: an approach using geographically weighted regression. *International journal of climatology* **21**(4): 455–466.

Carrivick JL, Brewer TR. 2004. Improving local estimations and regional trends of glacier equilibrium line altitudes. *Geografiska Annaler* **86**: 67–79.

Charlesworth JK. 1938. Some observations on the glaciation of north-east Ireland. *Proceedings of the Royal Irish Academy. Section B: Biological, Geological, and Chemical Science* **45**: 255–295.

Clark CD, Hughes AL, Greenwood SL, Jordan C, Sejrup HP. 2012. Pattern and timing of retreat of the last British-Irish Ice Sheet. *Quaternary Science Reviews* **44**: 112–146.

Colhoun EA, Synge FM. 1980. The cirque moraines at Lough Nahanagan, County Wicklow, Ireland. *Proceedings of the Royal Irish Academy. Section B: Biological, Geological, and Chemical Science* **80**B: 25–45.

Cooper MR, Johnston TP. 2004. Palaeogene Intrusive Igneous Rocks. In *The Geology of Northern Ireland, Our Natural Foundation*, Mitchell W (ed.). The Geological Survey of Northern Ireland: Belfast; 179–198.

Cornish R. 1981. Glaciers of the Loch Lomond Stadial in the western Southern Uplands of Scotland. *Proceedings of the Geologists Association* **92**: 105–114.

Dortch JM, Hughes PD, Tomkins MD. 2016. Schmidt Hammer exposure dating (SHED): Calibration boulder of Tomkins et al. (2016). *Quaternary Geochronology* **35**: 67–68.

Dortch JM, Owen LA, Caffee MW. 2013. Timing and climatic drivers for glaciation across semi-arid western Himalayan–Tibetan orogen. *Quaternary Science Reviews* **78**: 188–208.

Dwerryhouse AR. 1923. The glaciation of north-eastern Ireland. Quarterly Journal of the Geological Society **79**(1-4): 352–422.

Fairbanks RG. 1990. The age and origin of the "Younger Dryas climate event" in Greenland ice cores. *Paleoceanography* **5**(6): 937–948.

Gellatly AF. 1985. Introduction to the glacial history of the Mourne Mountains. In *1st International conference on geomorphology, Northern Ireland Fieldtrip*, Whalley WB, Smith BJ, Orford JD, Carter RWG (eds). Queen's University of Belfast Department of Geography.

Golledge NR. 2008. Glacial Geology and Glaciology of the Younger Dryas Ice Cap in Scotland (Unpublished PhD thesis). University of Edinburgh.

Golledge NR. 2010. Glaciation of Scotland during the Younger Dryas: a review. *Journal of Quaternary Science* **25**: 550–566.

Golledge NR, Hubbard AL, Bradwell T. 2010. Influence of seasonality on glacier mass balance, and implications for palaeoclimate reconstructions. *Climate Dynamics* **35**: 757–770.

Gordon JE. 1999. Loch Skene: Loch Lomond Readvance moraine system. In *The Quaternary of Dumfries and Galloway: Field Guide*, Tipping RM (ed.). Quaternary Research Association: London; 164–167.

Goudie AS. 2006. The Schmidt Hammer in geomorphological research. *Progress in Physical Geography* **30**: 703–718.

GSI, Geological Survey of Ireland, 1:500,000 Bedrock Geology of Ireland. 2016. http://www.dccae.gov.ie/natural-resources/en-ie/Geological-Survey-of-Ireland/Pages/Data-Downloads.aspx [2 August 2016].

Harrison S, Glasser N, Anderson E, Ivy-Ochs S, Kubik PW. 2010. Late Pleistocene mountain glacier response to North Atlantic climate change in southwest Ireland. *Quaternary Science Reviews* **29**(27): 3948–3955.

Hughes PD. 2009. Loch Lomond Stadial (Younger Dryas) glaciers and climate in Wales. *Geological Journal* **44**: 375–391.

Hughes PD, Braithwaite RJ. 2008. Application of a degree-day model to reconstruct Pleistocene glacial climates. *Quaternary Research* **69**: 110–116.

Imbrie J, Hays JD, Martinson DG, McIntyre A, Mix AC, Morley JJ, Pisias NG, Prell WL, Shackleton NJ. 1984. The orbital theory of Pleistocene climate: Support from a revised chronology of the marine $\delta^{18}O$ record. In *Milankovitch and Climate*, Vol. Series C, 126, Berger A et al. (ed.). NATO ASI, Springer: Berlin; 269–305.

Isarin RFB, Renssen H. 1999. Reconstructing and modelling late Weichselian climates: the Younger Dryas in Europe as a case study. *Earth-Science Reviews* **48**: 1–38.

Isarin RFB, Renssen H, Vandenberghe J. 1998. The impact of the North Atlantic Ocean on the Younger Dryas climate in northwestern and central Europe. *Journal of Quaternary Science* **13**(5): 447–453.

Kern Z, László P. 2010. Size specific steady-state accumulation-area ratio: an improvement for equilibrium-line estimation of small palaeoglaciers. *Quaternary Science Reviews* **29**: 2781–2787.

Laumann T, Reeh N. 1993. Sensitivity to climate change of the mass balance of glaciers in southern Norway. *Journal of Glaciology* **39**: 656–665.

Liu Z, Carlson AE, He F, Brady EC, Otto-Bliesner BL, Briegleb BP, Wehrenberg M, Clark PU, Wu S, Cheng J, Zhang J. 2012. Younger Dryas cooling and the Greenland climate response to CO_2. *Proceedings of the National Academy of Sciences* **109**(28): 11101–11104.

Lowe JJ, Rasmussen SO, Björck S, Hoek WZ, Steffensen JP, Walker MJC, Yu ZC, the INTIMATE group. 2008. Synchronisation of palaeoenvironmental events in the North Atlantic region during the Last Termination: a revised protocol recommended by the INTIMATE group. *Quaternary Science Reviews* **27**: 6–17.

Lukas S. 2006. *Morphostratigraphic principles in glacier reconstruction - a perspective from the British Younger Dryas*. Progress in Physical Geography **30**: 719–736.

Lukas S, Bradwell T. 2010. Reconstruction of a Lateglacial (Younger Dryas) mountain ice field in Sutherland, northwestern Scotland, and its palaeoclimatic implications. *Journal of Quaternary Science* **25**: 567–580.

Matthews JA, Shakesby R. 1984. The status of the "Little Ice Age"in southern Norway: relative-age dating of Neoglacial moraines with Schmidt hammer and lichenometry. *Boreas* **13**: 333–346.

Matthews JA, Owen G. 2010. Schmidt hammer exposure-age dating: developing linear age-calibration curves using Holocene bedrock surfaces from the Jotunheimen-Jostedalsbreen regions of southern Norway. *Boreas* **39**: 105–115.

McCabe AM, Clark PU. 1998. Ice-sheet variability around the North Atlantic Ocean during the last deglaciation. *Nature* **392**: 373–377.

McCabe AM, Clark PU, Clark J, Dunlop P. 2007. Radiocarbon constraints on readvances of the British–Irish Ice Sheet in the northern Irish Sea Basin during the last deglaciation. *Quaternary Science Reviews* 26(9): 1204–1211.

McCabe M, Dunlop P. 2006. *The Last Glacial Termination in Northern Ireland*. Geological Survey of Northern Ireland. Geological Survey of Northern Ireland: Belfast.

McCabe AM, Williams GD. 2012. Timing of the East Antrim Coastal Readvance: phase relationships between lowland Irish and upland Scottish ice sheets during the Last Glacial Termination. *Quaternary Science Reviews* **58**: 18–29.

Mitchell, WA. 1996. The significance of snowblow in the generation of Loch Lomond Stadial (Younger Dryas) glaciers in the western Pennines, northern England. *Journal of Quaternary Science* **11**: 233–248.

Murari MK, Owen LA, Dortch JM, Caffee MW, Dietsch C, Fuchs M, Haneberg WC, Sharma MC, Townsend-Small A. 2014. Timing and climatic drivers for glaciation across monsoon-influenced regions of the Himalayan–Tibetan orogen. *Quaternary Science Reviews* **88**: 159–182.

Ohmura A, Kasser P, Funk M. 1992. Climate at the equilibrium line of glaciers. *Journal of Glaciology* **38**(130): 397–411.

Osmaston H. 2005. Estimates of glacier equilibrium line altitudes by the Area × Altitude, the Area × Altitude Balance Ratio and the Area × Altitude Balance Index methods and their validation. *Quaternary International* **138–139**: 22–31

Pellitero R, Rea BR, Spagnolo M, Bakke J, Hughes P, Ivy-Ochs S, Lukas S, Ribolini A. 2015. A GIS tool for automatic calculation of glacier equilibrium-line altitudes. *Computers & Geosciences* **82**: 55-62.

Pellitero R, Rea BR, Spagnolo M, Bakke J, Ivy-Ochs S, Frew CR, Hughes P, Ribolini A, Lukas S, Renssen H. 2016. Glare, a GIS tool to reconstruct the 3D surface of palaeoglaciers. *Computers & Geosciences* **94**: 77–85.

Peterson TC, Vose RS. 1997. An overview of the Global Historical Climatology Network temperature database. *Bulletin of the American Meteorological Society* **78**(12): 2837–2849.

Porter SC. 2001. Snowline depression in the tropics during the Last Glaciation. *Quaternary Science Reviews* **20**: 1067–1091.

Rea BR, 2009. Defining modern day Area-Altitude Balance Ratios (AABRs) and their use in glacier-climate reconstructions. *Quaternary Science Reviews* **28**: 237–248.

Rea BR, McCarron S. 2008. The Younger Dryas in the North of Ireland. In *North of Ireland: Field Guide*, Whitehouse NJ, Roe HM, McCarron S, Knight J (eds). Quaternary Research Association: London.

Renssen H, Isarin RFB. 1998. Surface temperature in NW Europe during the Younger Dryas: AGCM simulation compared with temperature reconstructions. *Climate Dynamics* **14**: 33–44.

Renssen H, Vandenberghe J. 2003. Investigation of the relationship between permafrost distribution in NW Europe and extensive winter sea-ice cover in the North Atlantic Ocean during the cold phases of the Last Glaciation. *Quaternary Science Reviews* **22**: 209–223.

Renssen H, Mairesse A, Goosse H, Mathiot P, Heiri O, Roche DM, Nisancioglu KH, Valdes PJ. 2015. Multiple causes of the Younger Dryas cold period. Nature Geoscience **8**: 946–950.

Sissons JB, 1979. Palaeoclimatic inferences from former glaciers in Scotland and the Lake District. *Nature* **278**: 518–521.

Sissons JB. 1980. The Loch Lomond Advance in the Lake District, northern England. *Transactions of the Royal Society of Edinburgh: Earth Sciences* **71**: 13–27.

Stephens N, Creighton JR, Hannon MA. 1975. The Late-Pleistocene period in north-eastern Ireland: an assessment 1975. *Irish Geography* **8**(1): 1–23.

Sutton B. 1998. Glacial Landforms and Sedimentology, and Late Pleistocene Evolution of the Mourne Mountains, Northern Ireland. Unpublished PhD thesis, University of Ulster.

Tomkins MD, Dortch JM, Hughes PD. 2016. Schmidt Hammer exposure dating (SHED): Establishment and implications for the retreat of the last British Ice Sheet. *Quaternary Geochronology* **33**: 46–60.

Walker MJC. 2004. A Lateglacial pollen record from Hallsenna Moor, near Seascale, Cumbria, NW England, with evidence for arid conditions during the Loch Lomond (Younger Dryas) Stadial and early Holocene. *Proceedings of the Yorkshire Geological and Polytechnic Society* **55**(1): 33–42.

Walker MJC, Coope GR, Sheldrick C, Turney CSM, Lowe JJ, Blockley SPE, Harkness DD. 2003. Devensian Lateglacial environmental changes in Britain: a multi-proxy environmental record from Llanilid, South Wales, UK. *Quaternary Science Reviews* **22**: 475–520.

Walker MJC, Lowe J, Blockley SP, Bryant C, Coombes P, Davies S, Hardiman M, Turney CS, Watson J. 2012. Lateglacial and early Holocene palaeoenvironmental 'events' in Sluggan Bog, Northern Ireland: comparisons with the Greenland NGRIP GICC05 event stratigraphy. *Quaternary Science Reviews* **36**: 124–138.

Watson JE, Brooks SJ, Whitehouse NJ, Reimer PJ, Birks HJB, Turney C. 2010. Chironomid-inferred late-glacial summer air temperatures from Lough Nadourcan, Co. Donegal, Ireland. *Journal of Quaternary Science* **25**(8): 1200–1210.

Wilson KR. 2004a. The last glaciation in the western Mourne Mountains, Northern Ireland. *The Scottish Geographical Magazine* **120**(3): 199–210.

Wilson P. 2004b. Evidence for and reconstruction of a Nahanagan Stade glacier at Croloughan Lough, Derryveagh mountains, Co. Donegal. *Irish Journal of Earth Sciences* **22**: 45–54.

Winkler S. 2009. First attempt to combine terrestrial cosmogenic nuclide (10Be) and Schmidt hammer relative-age dating: Strauchon Glacier, Southern Alps, New Zealand. *Open Geosciences* **1**(3): 274–290.

Table 1. The peak age, 1σ uncertainties and P-values from T-Test between landform types at 2σ. P-values represent the relationship between the landform type they are listed across from and the next youngest in the table.

Landform	Selected Gaussian age (Ka)	P-values between 2σ Gaussian ages
Summit	15.6 ± 1.9	«0.01
Col	14.2 ± 1.7	«0.01
Valley	10.5 ± 1.4	«0.01
Cirque	8.8 ± 0.8	N/A

Table 2. Attributes (including ELA estimates) of reconstructed Younger Dryas glaciers in the Mournes.

Glacier number	Glacier/Cirque name	Lat (°N)	Lon (°W)	Area min/max (km²)	Z_{min} min/max (m.a.s.l.)	Z_{max} min/max (m.a.s.l.)	ELA (AABR: 1.9 ± 0.81) (m.a.s.l.)

1	Shanlieve	54.121	6.088	0.18/0.52	287/217	476/478	356 ± 33
2	Eagle Mountain (min/max)	54.136	6.089	0.05/0.10	348/320	503/507	403 ± 9
3	Slieve Muck	54.153	6.037	0.20/0.37	405/331	592/611	483 ± 30
4	Carn Mountain (min/max)	54.162	6.033	0.10/0.23	451/410	604/612	524 ± 14
5	Lough Shannagh	54.170	6.018	0.39	408	561	471 ± 8
6	OTT Mountain	54.176	6.024	0.07	440	551	507 ± 5
7	Slieve Meelbeg	54.187	6.006	0.07/0.11	485/449	617/618	546 ± 19
8	Pollaphuca	54.189	5.994	0.12/0.15	404/403	666/668	523 ± 25
9	Hare's Gap North	54.192	5.976	0.08	335	450	398 ± 6
10	Hare's Gap South	54.191	5.967	0.13/0.19	383/362	536/543	456 ± 10
11	Spinkwee Valley	54.194	5.954	0.21	331	536	430 ± 12
12	Pot of Legawherry	54.191	5.946	0.11/0.17	458/420	653/659	546 ± 14
13	Shan Slieve	54.193	5.941	0.03/0.06	515/476	624/626	563 ± 16
14	Pot of Pulgrave	54.192	5.934	0.05	503	664	570 ± 9
15	Glen River (min/max)	54.185	5.930	0.11/0.15	427/408	585/590	498 ± 14
16	Eagle Rock (min/max)	54.188	5.919	0.11/0.16	414/410	664/668	506 ± 15
17	Thomas' Mountain	54.189	5.910	0.14	433	597	524 ± 9
18	Crossone (min/max)	54.182	5.905	0.25/0.37	362/339	578/591	465 ± 16
19	Chimney Rock Mountain (min/max)	54.167	5.914	0.14/0.20	437/380	668/669	539 ± 36
20	Rocky Mountain	54.162	5.926	0.29	386	530	468 ± 6
21	Castles of Commedagh	54.180	5.939	0.16	400	548	478 ± 7
22	Cove Lough (min/max)	54.172	5.956	0.12/0.37	446/436	600/629	530 ± 16
23	Slievelamagan	54.166	5.961	0.07/0.16	466/389	699/700	528 ± 63
24	Binnian Lough	54.150	5.977	0.24	453	649	544 ± 10
	Mean						**475 ± 36**

Table 3. Reconstructed annual accumulation in the Mournes during the Younger Dryas, based on a mean 'climatic' ELA estimate from reconstructed glaciers. Accumulation estimates are calculated using a degree-day model (see section 3.5).

Mean 'climatic' ELA (m.a.s.l.)	Lapse rate (°C m^{-1})	DDF (mm °C^{-1} day^{-1})	Accumulation at ELA (mm a^{-1})
529 ± 4	0.006	2.6	984 ± 6
529 ± 4	0.007	2.6	851 ± 7
529 ± 4	0.006	4.1	1551 ± 10
529 ± 4	0.007	4.1	1343 ± 11
529 ± 4	0.006	5.6	2119 ± 13
529 ± 4	0.007	5.6	1834 ± 24

Supplementary information

Supp 1. Schmidt hammer data from the Mourne Mountains. R-values, age estimates, and their uncertainties represent the mean and mean absolute deviation of 30 measurements per sample site. Numbered locations are shown in Fig. 1A.

Location number	Location classification	Sample	Latitude (°N)	Longitude (°W)	Sample type	Altitude (m.a.s.l.)	R-value	R-value Uncertainty	Age (ka)	Age uncertainty calibration curve (ka)	Total Uncertainty propagated quadratically (ka)
1	Cirque	1	54.1696	5.9124	Boulder	415	56.1	1.6	7.5	1.60	1.61
		2	54.1693	5.9124	Boulder	423	54.2	1.7	8.4	1.60	1.62
		3	54.1686	5.9122	Boulder	449	56.7	1.9	7.2	1.60	1.61
2	Cirque	1	54.1217	6.0869	Boulder	303	54.6	1.7	8.2	1.60	1.62
		2	54.1215	6.0866	Boulder	297	56.5	1.6	7.2	1.60	1.61
		3	54.1216	6.0865	Boulder	296	55.5	1.7	7.7	1.60	1.61
3	Cirque	1	54.1518	5.9721	Boulder	454	57.3	2	6.9	1.60	1.61
		2	54.1506	5.9675	Boulder	451	52.8	2.5	9	1.60	1.65
		3	54.1497	5.9663	Boulder	447	55.8	2.6	7.6	1.60	1.63
4	Cirque	1	54.1362	6.0894	Boulder	359	53.6	1.4	8.7	1.60	1.61
		2	54.136	6.0887	Boulder	355	56	1.2	7.5	1.60	1.60
		3	54.1356	6.0882	Boulder	352	55.7	1.6	7.7	1.60	1.61
5	Cirque	1	54.1924	5.9488	Boulder	448	58	1.6	6.5	1.60	1.61
		2	54.1927	5.9482	Boulder	437	54.2	1	8.4	1.60	1.60
		3	54.1931	5.9464	Boulder	440	52.5	1.4	9.2	1.60	1.61
6	Cirque	1	54.1785	6.0302	Boulder	406	55.2	0.9	7.9	1.60	1.60
		2	54.1777	6.0288	Boulder	430	55.6	1.2	7.7	1.60	1.60
		3	54.1775	6.0254	Boulder	455	53.7	1	8.6	1.60	1.60
7	Cirque	1	54.1671	5.9556	Boulder	453	57	1.9	7	1.60	1.61
		2	54.1668	5.9543	Boulder	450	53.3	2.9	8.8	1.60	1.67
		3	54.1673	5.9506	Boulder	423	53.2	1.7	8.9	1.60	1.62
8	Cirque	1	54.1585	6.027	Boulder	353	51.4	2.2	9.7	1.60	1.65
		2	54.1585	6.0254	Boulder	362	54.9	1.2	8	1.60	1.61
		3	54.1426	6.0125	Boulder	370	56.9	0.9	7	1.60	1.60
9	Cirque	1	54.1925	5.9779	Boulder	351	54.2	1.6	8.4	1.60	1.62
		2	54.1928	5.9788	Boulder	343	55.3	1.2	7.8	1.60	1.61
		3	54.1938	5.9788	Boulder	337	53.6	1.7	8.7	1.60	1.62
10	Cirque	1	54.1378	6.0894	Boulder	360	55.7	1.5	7.7	1.60	1.61
		2	54.1371	6.0886	Boulder	337	53.1	1.7	8.9	1.60	1.62
		3	54.1371	6.0895	Boulder	351	54	1.5	8.5	1.60	1.61
11	Cirque	1	54.1874	5.9288	Boulder	428	52.6	1.8	9.2	1.60	1.63
		2	54.1867	5.9296	Boulder	440	55.9	1.1	7.5	1.60	1.60
		3	54.1867	5.9296	Boulder	439	53.1	1.2	8.9	1.60	1.61
12	Cirque	1	54.1912	6.0137	Boulder	395	52.8	2.2	9.1	1.60	1.64

		2	54.1901	6.0121	Boulder	425	52.2	1.9	9.4	1.60	1.63
		3	54.1909	6.0128	Boulder	405	56.2	2.2	7.4	1.60	1.62
13	Cirque	1	54.1784	5.9397	Boulder	423	53.1	1	8.9	1.60	1.60
		2	54.1776	5.9415	Boulder	391	53.3	1.4	8.8	1.60	1.61
		3	54.1785	5.9418	Boulder	401	54.7	1.5	8.1	1.60	1.61
14	Cirque	1	54.1922	5.932	Boulder	506	52.5	1.4	9.2	1.60	1.61
		2	54.1924	5.932	Boulder	512	53.6	1.8	8.7	1.60	1.62
		3	54.1927	5.9322	Boulder	522	54.9	1	8	1.60	1.60
15	Cirque	1	54.1216	6.0808	Boulder	252	53.4	1.3	8.7	1.60	1.61
		2	54.1216	6.081	Boulder	254	51.4	2.3	9.8	1.60	1.66
		3	54.1213	6.0811	Boulder	258	55.5	0.9	7.7	1.60	1.60
16	Col	1	54.1543	6.1093	Boulder	348	51.9	1.5	9.5	1.60	1.62
		2	54.1553	6.1085	Boulder	349	56.9	1.2	7.1	1.60	1.60
		3	54.1555	6.1079	Boulder	351	51.5	1.3	9.7	1.60	1.61
17	Valley	1	54.1828	6.0372	Boulder	382	54.7	2.1	8.1	1.60	1.63
		2	54.1816	6.0377	Boulder	410	53.2	3	8.9	1.60	1.67
		3	54.1807	6.0343	Boulder	385	51.7	1.3	9.6	1.60	1.61
18	Cirque	1	54.1523	6.0359	Boulder	422	50.5	1.1	10.2	1.60	1.61
		2	54.1522	6.036	Boulder	426	52.2	1.4	9.4	1.60	1.62
		3	54.1522	6.0356	Boulder	418	55.9	1.3	7.6	1.60	1.61
19	Valley	1	54.1475	6.0343	Boulder	338	51.3	1.8	9.8	1.60	1.63
		2	54.1471	6.0337	Boulder	331	56.3	2	7.3	1.60	1.62
		3	54.1472	6.0348	Boulder	335	50.5	1.4	10.2	1.60	1.62
20	Col	1	54.1476	6.0941	Surface	404	50.9	1.3	10	1.60	1.62
		2	54.1477	6.093	Surface	411	56.3	1.7	7.4	1.60	1.61
		3	54.1476	6.0926	Surface	412	50.9	1.3	10	1.60	1.62
21	Cirque	1	54.191	5.9891	Boulder	398	53.8	2.2	8.6	1.60	1.63
		2	54.1917	5.9887	Boulder	384	44.8	1.5	13	1.52	1.59
		3	54.1917	5.9886	Boulder	357	57.8	1.3	6.6	1.60	1.60
22	Summit	1	54.1496	6.1123	Surface	438	51.9	1.3	9.5	1.60	1.61
		2	54.1499	6.1122	Surface	437	53.2	1.2	8.9	1.60	1.61
		3	54.15	6.1122	Surface	436	51.2	1.6	9.8	1.60	1.63
23	Valley	1	54.16	6.1169	Boulder	262	51.7	1.2	9.6	1.60	1.61
		2	54.1598	6.1182	Boulder	266	53.1	1.7	8.9	1.60	1.62
		3	54.1602	6.1164	Boulder	267	51.1	1.2	9.9	1.60	1.61
24	Valley	1	54.1317	6.0786	Boulder	212	52	1.3	9.5	1.60	1.61
		2	54.1322	6.0776	Boulder	201	52.4	1.7	9.3	1.60	1.62

		3	54.1322	6.0774	Boulder	202	48.9	1.3	11	1.53	1.55
25	Valley	1	54.1447	6.0246	Boulder	269	50.3	1.3	10.3	1.60	1.62
		2	54.1451	6.0241	Boulder	266	52.7	1.8	9.1	1.60	1.63
		3	54.1457	6.0234	Boulder	274	48.5	1.6	11.2	1.57	1.61
26	Summit	1	54.1216	6.0935	Boulder	486	51.6	1.8	9.6	1.60	1.63
		2	54.1216	6.0937	Boulder	488	50.8	1.6	10	1.60	1.63
		3	54.1215	6.0937	Boulder	489	49	1.8	10.9	1.58	1.63
27	Col	1	54.1737	6.0228	Surface	514	55.3	1.2	7.9	1.60	1.61
		2	54.1742	6.0222	Boulder	510	49.6	1.4	10.6	1.59	1.61
		3	54.1741	6.022	Boulder	511	46.4	3.4	12.2	1.54	1.78
28	Valley	1	54.1947	5.9173	Boulder	287	49.4	4.1	10.7	1.58	1.82
		2	54.1927	5.9217	Boulder	308	48.3	2.1	11.3	1.57	1.64
		3	54.1926	5.9216	Boulder	315	52.8	1.3	9.1	1.60	1.61
29	Valley	1	54.1587	5.9731	Boulder	352	52.3	1.7	9.3	1.60	1.62
		2	54.1577	5.9648	Boulder	341	49.7	2	10.6	1.59	1.64
		3	54.1579	5.9618	Boulder	337	47.5	2.1	11.6	1.56	1.64
30	Valley	1	54.1566	5.9586	Boulder	295	49.9	2	10.5	1.59	1.65
		2	54.1566	5.9585	Boulder	294	49.3	1.9	10.8	1.58	1.64
		3	54.1564	5.9585	Boulder	293	47.5	2.2	11.6	1.56	1.65
31	Valley	1	54.1718	5.8921	Boulder	211	52.1	1.7	9.4	1.60	1.63
		2	54.172	5.8925	Boulder	209	49.4	2	10.7	1.58	1.64
		3	54.1718	5.8927	Boulder	216	45.1	1.5	12.8	1.53	1.59
32	Cirque	1	54.1679	6.0143	Boulder	413	51.6	1.9	9.6	1.60	1.63
		2	54.1662	6.0164	Boulder	418	53.3	1.2	8.8	1.60	1.61
		3	54.1641	6.0196	Boulder	413	39.9	1.4	15.3	1.50	1.59
33	Summit	1	54.1895	6.0009	Boulder	685	53.9	2.3	8.5	1.60	1.64
		2	54.1903	6.001	Boulder	675	49	2.8	10.9	1.58	1.70
		3	54.1913	6.0004	Boulder	681	40.9	3	14.9	1.50	1.86
34	Col	1	54.1903	5.9731	Bouler	441	43.6	3.1	13.5	1.51	1.79
		2	54.1903	5.9734	Bouler	443	48.4	1.4	11.2	1.57	1.60
		3	54.1903	5.9735	Bouler	441	51.4	1.3	9.8	1.60	1.62
35	Valley	1	54.1954	6.0184	Boulder	330	48.7	2.8	11.1	1.57	1.70
		2	54.1954	6.0184	Boulder	332	47.5	2.1	11.6	1.56	1.64
		3	54.1954	6.0183	Boulder	333	43.4	2.2	13.6	1.51	1.66
36	Cirque	1	54.1898	5.929	Boulder	377	42.9	1.5	13.9	1.51	1.59
		2	54.1885	5.9282	Boulder	403	41.9	2.1	14.4	1.50	1.67
		3	54.1882	5.9278	Boulder	414	54.4	1.8	8.3	1.60	1.62

37	Summit	1	54.1404	5.971	Surface	648	44.7	1.6	13	1.52	1.59
		2	54.1404	5.9709	Surface	648	45.4	1.5	12.7	1.53	1.59
		3	54.1403	5.9709	Surface	649	49.1	2.1	10.9	1.58	1.65
38	Col	1	54.1722	5.9258	Bouler	529	46.3	2.3	12.2	1.54	1.66
		2	54.1729	5.927	Bouler	544	47.5	1.7	11.6	1.56	1.61
		3	54.1726	5.9282	Bouler	538	44.9	1.2	12.9	1.53	1.56
39	Valley	1	54.136	6.0321	Boulder	225	42.7	2.1	14	1.51	1.66
		2	54.136	6.032	Boulder	224	48.6	1.2	11.1	1.57	1.59
		3	54.1361	6.0331	Boulder	211	42.5	1.1	14.1	1.51	1.55
40	Summit	1	54.1676	5.919	Surface	604	41.9	1.5	14.4	1.50	1.59
		2	54.1672	5.919	Surface	614	47.1	2	11.8	1.55	1.63
		3	54.1674	5.9196	Surface	610	41.8	1.9	14.4	1.50	1.64
41	Col	1	54.1861	5.9962	Boulder	522	44.8	1.6	12.9	1.52	1.59
		2	54.1859	5.996	Boulder	517	43.7	2.2	13.5	1.52	1.66
		3	54.1859	5.9962	Boulder	521	42	1.7	14.3	1.51	1.61
42	Summit	1	54.1848	5.99	Surface	731	43.1	1.5	13.8	1.51	1.59
		2	54.1848	5.9898	Surface	730	45	1.9	12.9	1.53	1.62
		3	54.1839	5.989	Surface	728	41.1	1.4	14.8	1.50	1.58
43	Valley	1	54.1398	5.94	Boulder	182	39.3	0.9	15.6	1.50	1.54
		2	54.141	5.9439	Boulder	204	50.7	2.4	10.1	1.60	1.67
		3	54.1414	5.9468	Boulder	219	36.7	1.5	16.9	1.50	1.65
44	Summit	1	54.1534	5.9812	Surface	654	41.5	1.2	14.6	1.50	1.56
		2	54.1537	5.9802	Surface	675	45	2.5	12.9	1.53	1.69
		3	54.1536	5.9805	Surface	659	39.7	1.1	15.5	1.50	1.56
45	Col	1	54.1839	5.9337	Tor	576	42.6	1.7	14	1.51	1.61
		2	54.1839	5.9337	Tor	576	41.1	1.4	14.8	1.50	1.58
		3	54.1839	5.9337	Tor	575	41.1	2	14.8	1.50	1.67
46	Valley	1	54.2027	5.9943	Surface	253	40.6	1.8	15	1.50	1.64
		2	54.2028	5.9948	Surface	258	42.6	2.3	14	1.51	1.69
		3	54.2028	5.9947	Surface	257	40	1.9	15.3	1.50	1.67
47	Summit	1	54.1363	6.1	Surface	592	36.4	1.1	17.1	1.50	1.59
		2	54.1365	6.1003	Surface	598	40.5	1.6	15	1.50	1.61
		3	54.1365	6.1008	Surface	605	39.3	2.7	15.6	1.50	1.84
48	Summit	1	54.1756	5.9556	Surface	623	38.5	1.4	16	1.50	1.61
		2	54.1757	5.9551	Surface	627	40.8	1.7	14.9	1.50	1.62
		3	54.1758	5.9552	Surface	623	36.5	1.2	17	1.50	1.60
49	Summit	1	54.1588	6.0396	Boulder	662	38	1.6	16.3	1.50	1.65

		2	54.1589	6.0397	Boulder	661	39.3	2.3	15.7	1.50	1.76
		3	54.1586	6.04	Boulder	659	38.2	1.8	16.2	1.50	1.68
50	Summit	1	54.1673	6.029	Surface	585	37.1	1.2	16.7	1.50	1.60
		2	54.1672	6.0289	Surface	587	39.9	1.9	15.4	1.50	1.67
		3	54.1677	6.03	Surface	548	38.2	1.4	16.2	1.50	1.61
51	Summit	1	54.1651	5.9662	Surface	670	42.2	1.8	14.2	1.51	1.62
		2	54.1645	5.966	Surface	661	37.4	1.8	16.6	1.50	1.70
		3	54.1641	5.9657	Surface	654	35.6	1.3	17.5	1.51	1.64
52	Summit	1	54.1812	5.9201	Boulder	835	38.4	1.5	16.1	1.50	1.63
		2	54.1806	5.9212	Boulder	846	30.9	1	19.7	1.55	1.68
		3	54.1806	5.92	Boulder	844	41.8	1.8	14.4	1.50	1.63
53	summit	1	54.1417	5.98	Surface	746	30.3	2	20.1	1.57	2.05
		2	54.1427	5.98	Surface	747	41.4	2.3	14.6	1.50	1.71
		3	54.1446	5.9795	Surface	709	37.2	2.6	16.7	1.50	1.90
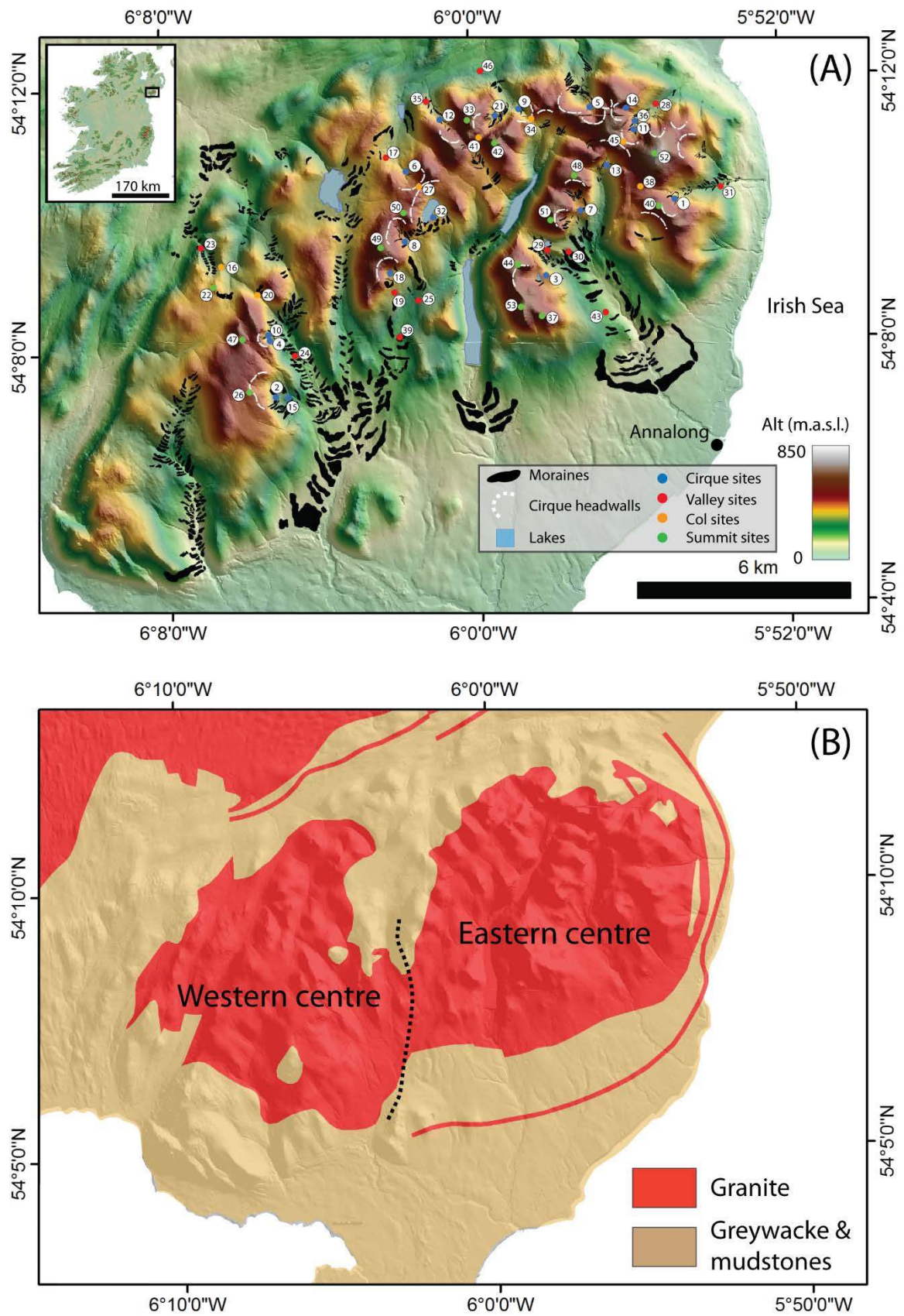
Figure 1. The Mourne Mountains, NE Ireland. (A) Geomorphological map. Sites mentioned in the legend refer to Schmidt hammer sampling locations, which are also numbered as in the Table S1. (B) Generalized geological map (GSI, 2016). The dashed line (in 'B') roughly marks the division between the Eastern Mournes (dominated by G1–G3 granites) and Western Mournes (dominated by G5 and G4 granites) (see Cooper and Johnston, 2004).
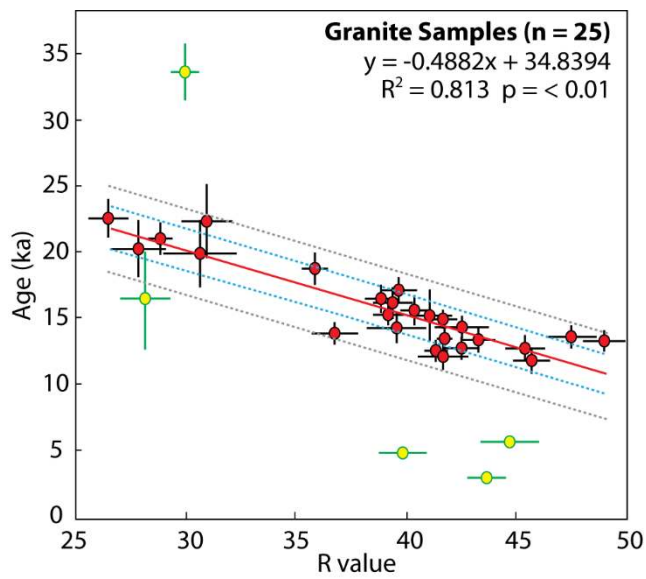
22

Figure 2. Schmidt hammer calibration curve for comsogenically dated granite boulders in the UK (curve developed by Tomkins et al., 2016). Here, R-values are plotted against ^{10}Be age. The regression line is shown in solid red. The blue and grey dashed lines denote one and two sigma boundaries, respectively. The data used to generate the regression line are shown as red dots with black error bars. Outliers, excluded from the calibration, are shown as yellow dots with green error.
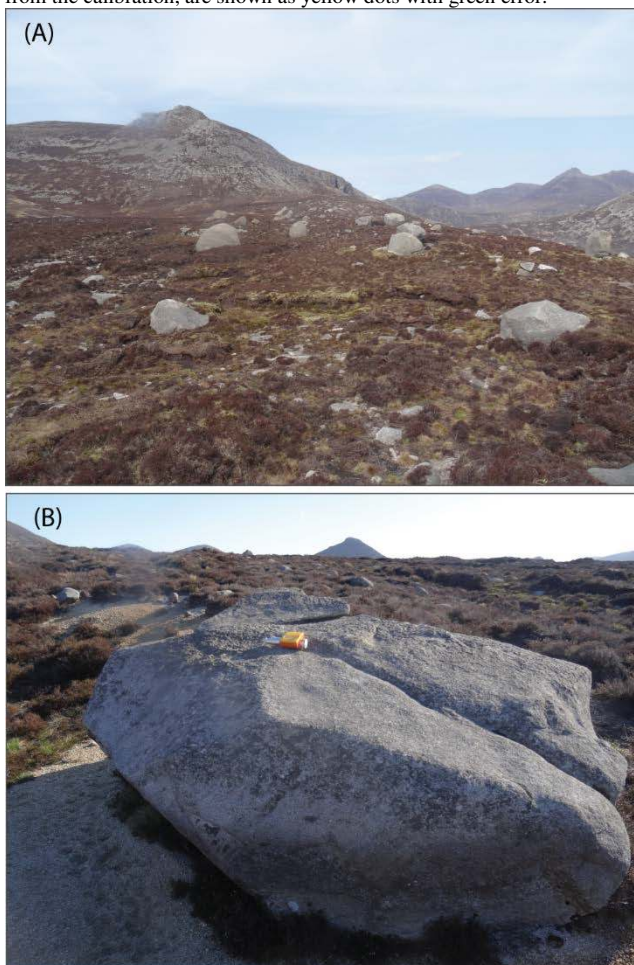
Figure 3. Examples of moraine crest boulder samples for Schmidt hammer exposure dating. (A) At Binnian Lough Corrie (54.151°N, 5.969°W). (B) At Carn Mountain Corrie (54.154°N, 6.026°W).
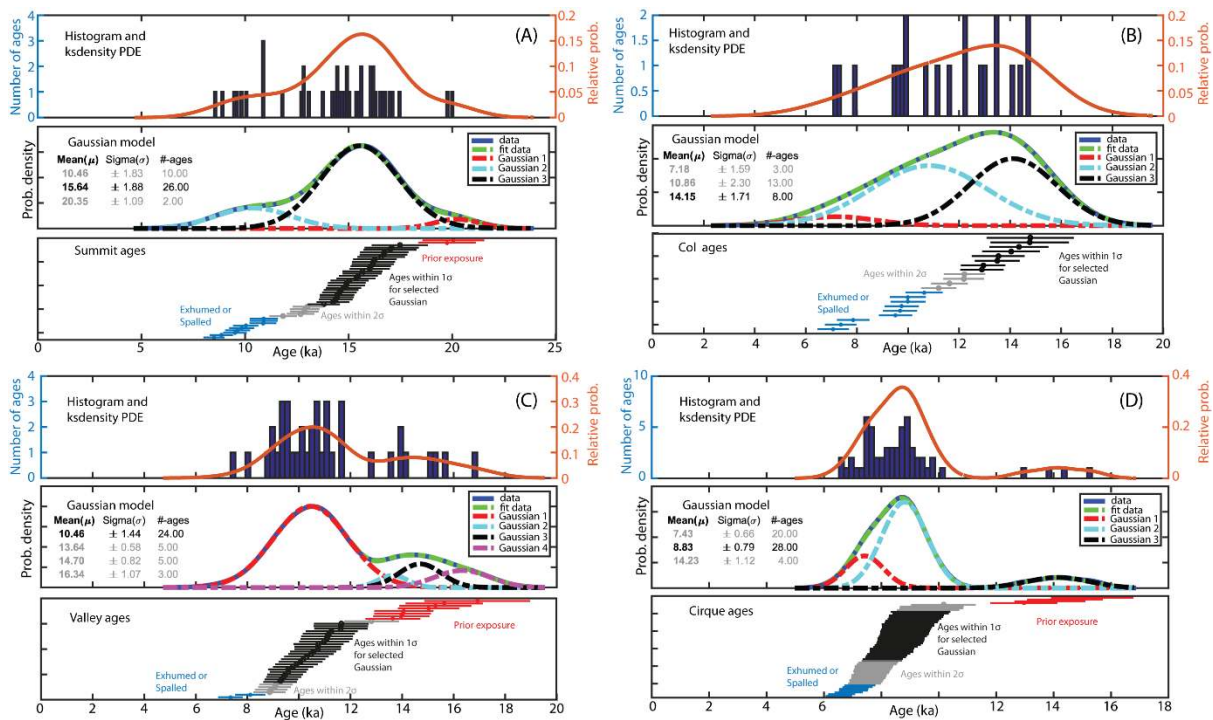
Figure 4. Probability density estimates and Gaussian models showing a distinction between ages [from: (A) summit (15.6_1.9 ka), (B) col (14.2_1.7 ka), (C) valley (10.5_1.4 ka) and (D) cirque (8.8_0.8 ka) locations].
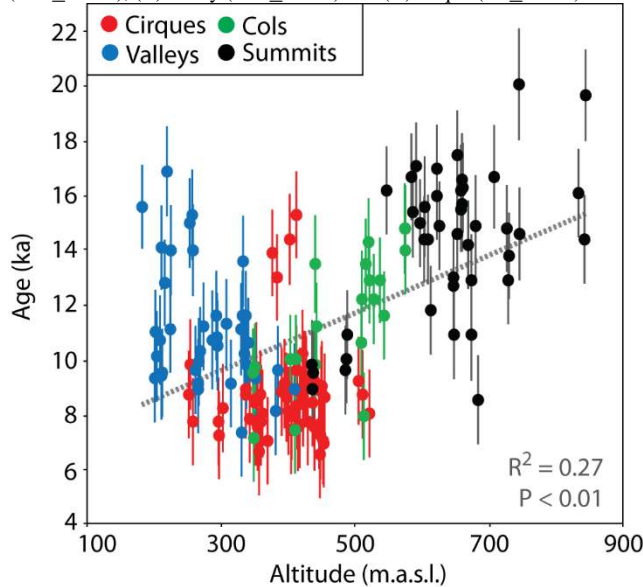

Figure 5. SHED age estimates plotted against altitude. For each site, the dot represents the mean value (based on 30 R-values per sample site). Error bars represent the quadratic propagation of the absolute mean deviation of R-values (30 hits) and one-sigma uncertainty from calibration against the granite regression curve of Tomkins et al. (2016). The dashed regression line reflects the trend for the entire dataset. Data are presented in Table S1.
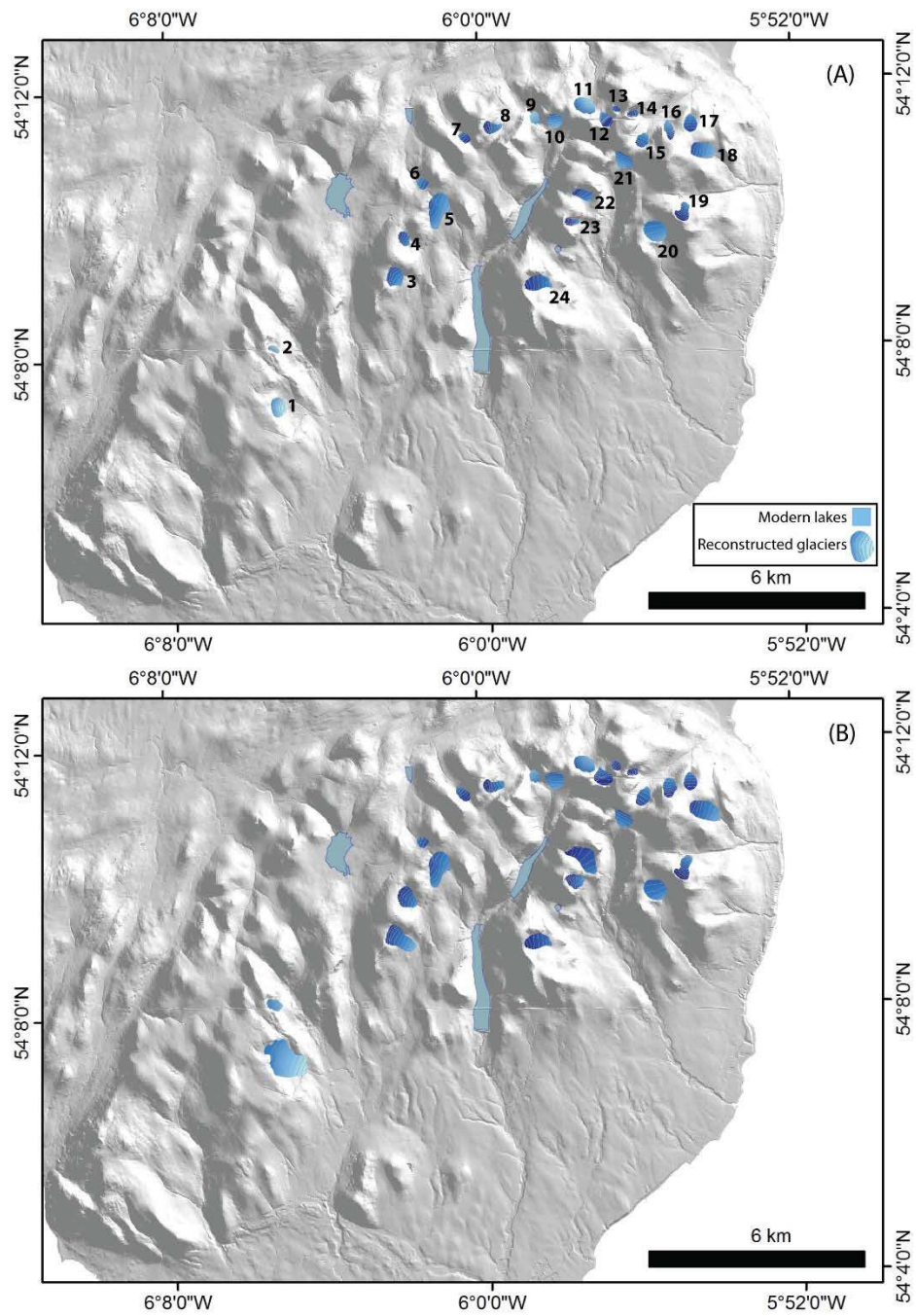
Figure 6. Minimum (A) and maximum (B) reconstructions of Younger Dryas glaciers in the Mournes. Glacier surfaces are contoured at 25-m intervals.
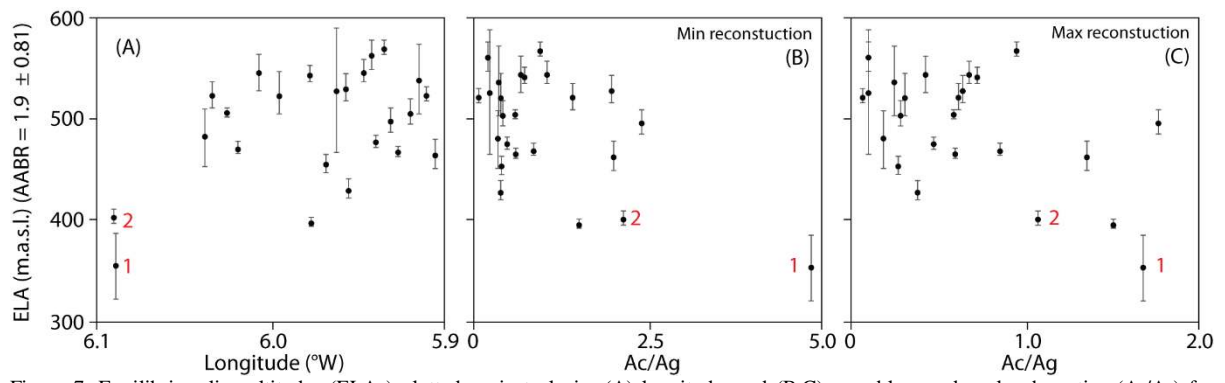
Figure 7. Equilibrium-line altitudes (ELAs) plotted against glacier (A) longitude, and (B,C) snowblow and avalanche ratios (A_c/A_g) for reconstructed Younger Dryas glaciers in the Mournes. Results from the minimum and maximum glacier reconstructions are shown in 'B' and 'C', respectively. Labels '1' and '2' refer to glaciers in the western Mournes (Fig. 6).